

## THE KINETICS OF VIBRATIONAL ENERGY TRANSFER AND RELAXATION PROCESSES IN MATRIX ISOLATED CH<sub>3</sub>F

V.A. APKARIAN and Eric WEITZ\*

*Department of Chemistry and Materials Research Center, Northwestern University, Evanston, Illinois 60201 USA*

Received 11 August 1980

Subsequent to exciting  $\nu_3$  by a CO<sub>2</sub> laser pulse, fluorescence has been detected from  $2\nu_3$  of CH<sub>3</sub>F trapped in rare gas matrices.  $2\nu_3$  is activated by V-V energy transfer and deactivates at twice the rate of  $\nu_3$  relaxation. A kinetic model is presented to interpret these observations.

### 1. Introduction

The study of vibrational relaxation and energy transfer processes in matrix isolated molecules has blossomed in the past few years. Information now exists on the behavior of a number of vibrationally and electronically excited matrix isolated species [1]. One such system is CH<sub>3</sub>F [2].

Vibrational energy transfer in CH<sub>3</sub>F isolated in rare gas matrices has previously been studied by a double resonance method where  $\nu_3$ , the C-F stretching mode, was pumped by a pulsed CO<sub>2</sub> laser and the time evolution of the  $\nu_3$  population probed by a cw CO<sub>2</sub> laser [2]. These experiments documented the relaxation processes in CH<sub>3</sub>F and furthered our understanding of vibrational relaxation of polyatomic molecules trapped in cryogenic matrices. However, due to their nature, the experiments shed little light on intermolecular V-V energy transfer simply because the monitored state is also the one that is initially excited. A study of intermolecular V-V energy transfer processes was the motivation for initiating studies of the same system via the technique of laser induced fluorescence, which has been widely applied to the gas phase. By means of this technique the time evolution of population in a state other than the initially excited state is normally monitored. In the above system, in a matrix, the only vibrational energy transfer pathway for populating

the monitored state is via intermolecular V-V transfer. Therefore, potentially, this technique could provide information not only about relaxation processes in the system under consideration but also about V-V equilibration steps.

CH<sub>3</sub>F is an ideal system for study by the laser induced fluorescence technique. The pump state,  $\nu_3$ , is the lowest in the manifold and all pathways for direct V-V energy transfer to other fundamentals are prohibitively endoergic. Thus, under these pump conditions, the only efficiently populated states are expected to be the overtones of  $\nu_3$  of which the first overtone transition has a large oscillator strength and is therefore readily observable. The experiment, therefore, selects out the  $\nu_3$  mode and its overtones from the rest of the vibrational manifold. This effective reduction in complexity of the system, simplifies interpretations and facilitates the treatment of the system's kinetics.

In what follows, only experiments performed in Kr and Xe matrices will be reported on and discussed in terms of a kinetic model. Only necessary allusions to the spectroscopy will be made leaving a more detailed interpretation of the high-resolution Fourier transform IR spectra of this system to a future publication.

### 2. Experimental

A diagram of the experimental apparatus is presented

\* Alfred P. Sloan Fellow.

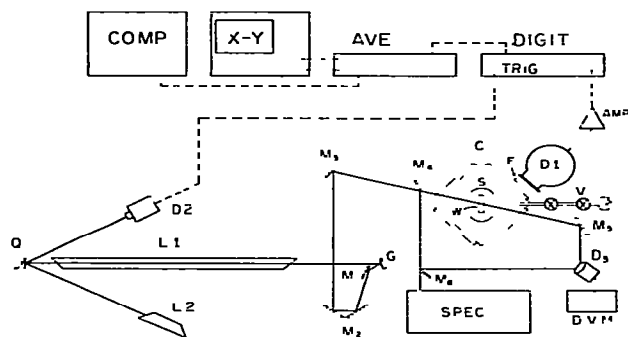


Fig. 1. Schematic of the experimental apparatus. The indicated symbols represent the following. C, cryostat; D1, InSb detector, D2, trigger photodiode, D3, power meter,  $\Gamma$ , interference filter, G, CO<sub>2</sub> laser grating, L1, CO<sub>2</sub> laser; L2, HeNe trigger laser; M1–M6, mirrors, Q, Q-switch mirror, S, cryoshroud, V, vacuum system for deposition, and W, sample window.

in fig. 1. An Air Products Displex 202 system was used as the cryostat. A CsI or sapphire window was used as a deposition substrate and salt windows were used for observation. The cryohead was connected to a glass vacuum system by 3/4" corrugated stainless steel tubing. Pressure was monitored at the cryohead by an ionization gauge and the temperature was monitored by a thermocouple gauge and a H<sub>2</sub> pressure gauge both of which were terminated at the copper block substrate mount. Samples were pulsed deposited through a 1/16 inch stainless steel tube which was kept at a distance of 1 inch from the substrate. The pulsed deposition was either controlled manually or by two serial solenoid valves. Pulse sizes varied from  $\approx 0.5$  to  $\approx 5$  Torr  $\ell$ . The reservoir pressure for the deposited gas varied between 300 and 500 Torr. During deposition a vacuum of better than  $10^{-6}$  Torr was maintained at the cryohead. When mechanically pulsed the repetition rate was 1 Hz. The entire system, cryostat and vacuum manifold could be made to access a Nicolet 7000 FTIR spectrometer via which high-resolution infrared spectra were recorded.

A 3 m transversely pumped CO<sub>2</sub> laser, Q switched by a rotating mirror and output coupled by a grating was used as the excitation source. While the output parameters of the laser varied in different experiments, typical values were: 2 mJ/pulse at 100 Hz repetition rate, 800 ns fwhm and 1 cm beam diameter. The experimental geometry was as shown in fig. 1. The geometry was varied slightly around the indicated positions to

maximize beam overlap with the matrix, minimize laser scatter and maximize detector collection of fluorescence from the matrix. The laser beam was not focused and overlapped almost the entire matrix. When sapphire was used as a deposition window the matrix was deposited on the same side as the incident laser beam otherwise it was deposited on the detector side of the matrix substrate.

In all experiments involving  $2\nu_3$  emission, either of two photovoltaic InSb detectors with sapphire windows were used to monitor fluorescence signals. Signals were preamplified and recorded by a transient recorder (Biomation 8100 or 610B) and then averaged. The averaged signals were displayed on an X–Y scope and sent to a computer (Nova 4, Nova 3, or CDC 6600) for analysis.

Most experiments were performed with a 4.8  $\mu\text{m}$  long pass filter interposed between the InSb detector and the cryohead. With this filter the effective band-pass of the detector becomes 4.83–5.67  $\mu\text{m}$  (5% points). In some experiments an OCLI circular variable filter was interposed between the detector and cryohead in an effort to accurately determine the wavelength region of the observed emission. With the 610B and the photovoltaic InSb detector A, the overall detection system and associated electronics had a response time of 0.6  $\mu\text{s}$ . With the photovoltaic InSb detector B and the Biomation 8100 transient recorder, the detection system and electronics had a response time of 0.3  $\mu\text{s}$ . While with the latter system, the response time was substantially faster, the detectivity was approximately an order of magnitude lower and thus this system was not routinely used.

Unsuccessful efforts were made to observe emission from other states, the photovoltaic InSb detector A and appropriate filters were used in an attempt to observe [ $\nu_1, \nu_4$ ] while a photoconductive AuGe detector and appropriate filters were used in an attempt to observe [ $\nu_2, \nu_5$ ] and  $\nu_6$ .

CH<sub>3</sub>F was obtained from Matheson and was subjected to multiple freeze–thaw cycles yielding a sample with a vapor pressure of  $5 \times 10^{-5}$  Torr at 77 K. The rare gases were obtained from Cryogenic Rare Gases and were used without further purification. Nominal purities were Kr, 99.999% and Xe, 99.999%. Samples were prepared on a metal vacuum system in either stainless steel or glass bulbs. Vessels were flamed under vacuum prior to filling. Samples of the desired M/R ratio were

prepared by successive dilution with rare gases. During these dilutions, pressure was measured by a capacitance manometer. Samples were allowed to mix for at least 12 h before usage.

All spectroscopic studies were done with a Nicolet 7000 Fourier transform spectrometer. This system is capable of  $0.06 \text{ cm}^{-1}$  resolution.

### 3. Results

FTIR spectra of  $\text{CH}_3\text{F}$  isolated in Kr and Xe matrices were recorded. The monomeric and dimeric  $\nu_3$  bands were identified by heat cycling studies in agreement with the previous assignments [2]. In a  $1000 \cdot 1, \approx 100 \mu\text{m}$  thick Xe matrix all other fundamentals were identified and most importantly  $2\nu_3$  was observed at  $2044 \text{ cm}^{-1}$ . In table 1, approximate band centers for all observed bands are reported along with their tentative assignments.

P(32) and P(36) of the  $9.6 \mu\text{m}$   $\text{CO}_2$  laser band overlap the monomeric  $\nu_3$  lines in Kr and Xe respectively. When excited with these lines, very strong emission is observed centered at  $2030 \pm 40 \text{ cm}^{-1}$ , as determined by an InSb detector and a circular variable filter. A typical signal is shown in fig. 2. The agreement of the emission band center with the observed absorption band at  $2044 \text{ cm}^{-1}$  is taken as proof that  $2\nu_3$  is the emitting state in these experiments. In all matrices, emission from all other fundamentals was searched for but not found. Thus only emission from  $2\nu_3$  is ob-

Table 1

State	Gas-phase symmetry	Energy ( $\text{cm}^{-1}$ )
$\nu_3$	$a_1$	1030
$\nu_6$	$e$	1177
$\nu_2$	$a_1$	1456 a)
$\nu_5$	$e$	
$2\nu_3$	$a_1$	2044
$2\nu_5, \nu_2 + \nu_5$	$e$	2902
$2\nu_5$	$a_1$ <sup>b)</sup>	2849
$2\nu_2$	$a_1$	2950
$\nu_1$	$a_1$	2998
$\nu_4$	$e$	

a) A broad feature  $7 \text{ cm}^{-1}$  fwhm.

b)  $\nu_1, 2\nu_2$  and  $a_1$  component of  $2\nu_5$  are expected to mix and show a Fermi splitting centered on the  $e$  component of  $2\nu_5$ . This results in two spectral features centered at the positions shown above.

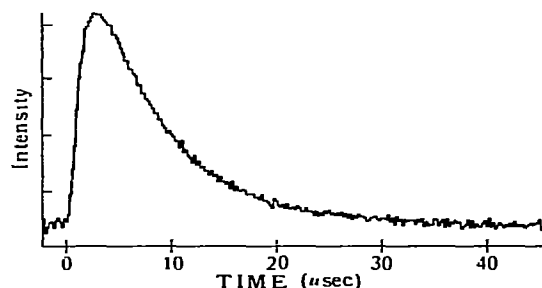


Fig. 2. Fluorescence signal from the  $2\nu_3$  mode of  $\text{CH}_3\text{F}$  for  $\text{CH}_3\text{F}$  isolated in a 15000 1M/R ratio Kr matrix at 12 K. The ordinate is in arbitrary intensity units.

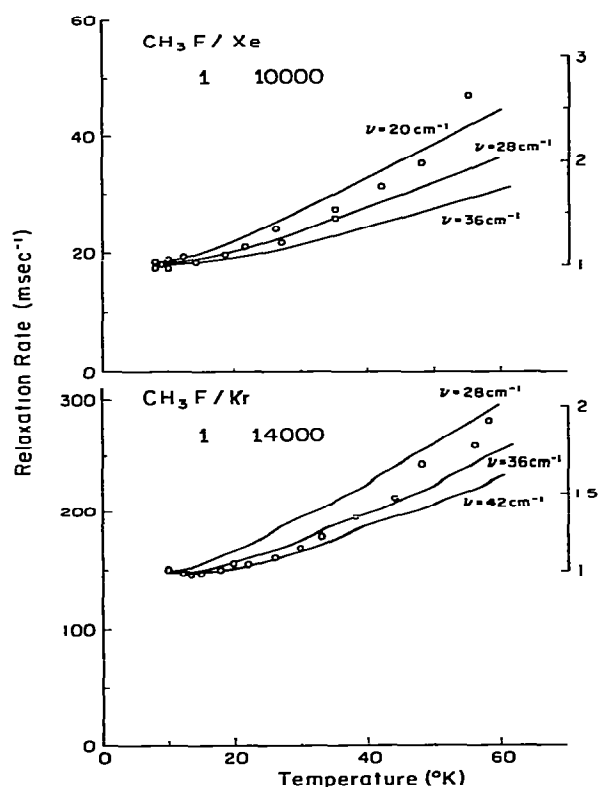
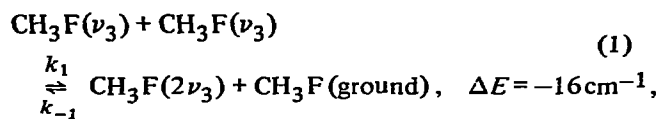


Fig. 3. The temperature dependence of the relaxation of  $2\nu_3$  in a 1:10000  $\text{CH}_3\text{F} \cdot \text{Xe}$  matrix (top) and in a 1:14000  $\text{CH}_3\text{F} \cdot \text{Kr}$  matrix (bottom). The experimental points ( $\circ$ ) are superimposed on the temperature dependence of the phonon population for phonons of energy  $\nu$  [7,8]. The relaxation rate (in ms) is indicated on the left-hand ordinate while the rate normalized to the rate at 10 K is indicated on the right-hand ordinate.

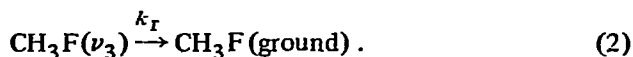
served in our experiments and the reported data pertain to this state. The rise and fall of the fluorescence signals from  $2\nu_3$  were monitored as a function of temperature for different  $M/R$  ratios in both Kr and Xe matrices. The temperature dependence of the fall rates in Kr and Xe are presented in fig. 3. The dependence of these rates upon excitation energy for a given set of conditions ( $M/R$  ratio, temperature and excitation lines) was tested by either spoiling the laser cavity or by inserting Ge windows in the beam. In the range of energies from 0.4 to 3.5 mJ/cm<sup>2</sup> no power dependence was observed in the fall rate. However, as will be further discussed in section 4, a power dependence is predicted for the rise rate and the behavior of the rise rate as a function of temperature and power contains a significant amount of information about the system's kinetics.

#### 4. Discussion

The temperature dependence of the deactivation rate of  $2\nu_3$ , depicted in fig. 3, is very similar to that reported for  $\nu_3$ . Furthermore, the absolute magnitude of the deactivation rate of  $2\nu_3$  is, within experimental error, twice that of  $\nu_3$ . The deactivation rate of  $\nu_3$  for a dilute ( $M/R > 10000 \cdot 1$ ) Kr matrix at 30 K was reported as  $87 \pm 4 \text{ ms}^{-1}$  and for a dilute Xe matrix, as  $18 \pm 2 \text{ ms}^{-1}$  [2,3]. We observe a deactivation rate for  $2\nu_3$  of  $180 \pm 10 \text{ ms}^{-1}$  in Kr and  $30 \pm 1 \text{ ms}^{-1}$  in Xe under similar conditions. This doubling of deactivation rate for  $2\nu_3$  relative to  $\nu_3$  can easily be rationalized on the basis of a sequential mechanism involving a bimolecular step for deactivating  $2\nu_3$



followed by



In such a mechanism, when the vibrational temperature is much greater than the bath temperature, which is virtually always the case for a laser excited species in a low-temperature matrix, the relaxation rate of the state  $\nu\nu_x$  will be  $\nu$  times the rate of state  $\nu_x$ , provided

that the initial activation rate to state  $\nu\nu_x$  is significantly faster than the relaxation rate of  $\nu_x$ ;  $k_1 \gg k_r$  [4]. Thus for the above case, where  $k_1$  approaches  $k_r$ , the fall rate of  $2\nu_3$  will slow down and approach  $k_r$ . For the case where  $k_1 < k_r$ ,  $2\nu_3$  would fall at a rate of  $k_{-1}$ .

Since  $2\nu_3$  deactivates at twice the rate of deactivation of  $\nu_3$  it can be concluded that the system's kinetics are compatible with bimolecular interactions on the deactivation timescale and additionally that  $k_1 \gg k_r$ . The latter conclusion is directly verified by the observation of a very fast rise for  $2\nu_3$  both in Xe and Kr (fig. 2).

In such a situation, where deactivation and V-V activation occur on relatively different timescales, the respective kinetic equations for the two steps [eqs. (1) and (2)] can be treated separately to yield an approximate analytical expression for the temporal behavior of each state. Thus solving eq. (1) for  $N_{2\nu_3}$  we obtain

$$N_{2\nu_3}(t) = N_{2\nu_3}^e \{1 - \exp[-(4k_1N_{\nu_3}^e + k_{-1})t]\}, \quad (3)$$

where  $N_{2\nu_3}^e$  and  $N_{\nu_3}^e$  are respectively the excess populations in  $2\nu_3$  and  $\nu_3$  after vibrational equilibrium. To incorporate a relaxation time for the population in  $2\nu_3$ , we simply take the solution for  $N_{\nu_3}(t)$  when eq. (2) is considered alone.

$$N_{\nu_3}(t) = \delta \exp(-k_r t), \quad (4)$$

where  $\delta$  is the fraction of molecules initially excited to  $\nu_3$  by the laser pulse, that are actually involved in V-V equilibration, and again solve the differential equation in eq. (1) for  $N_{2\nu_3}(t)$

$$N_{2\nu_3}(t) = N_{2\nu_3}^e \{ \exp(-2k_r t) - \exp[-(4k_1N_{\nu_3}^e + k_{-1})t] \}. \quad (5)$$

An expression for the relaxation of  $\nu_3$  can now be obtained taking into account the presence of  $2\nu_3$ . This yields

$$N_{\nu_3}(t) = N_{\nu_3}^e \exp[-(4k_1N_{\nu_3}^e + k_{-1})t] + (\delta - N_{2\nu_3}^e) \exp(-k_r t), \quad (6)$$

where the first exponential fall is simply due to population transfer from  $\nu_3$  to  $2\nu_3$  while the second is due to the overall deactivation step in the system. Indeed, a double exponential relaxation has been reported in

the fall of  $\nu_3$  in dilute matrices [2]. In order to quantify and completely evaluate the above expressions, the equilibrium populations,  $N^e$ , have to be solved for.

These equilibrium populations can be determined for a given bath temperature  $T_b$ , degree of excitation,  $\delta$ , and for a given equilibration mechanism by a consideration of the vibrational temperatures of the system [4]. For the mechanism of eqs. (1) and (2)

$$(E_{2\nu_3} - 2E_{\nu_3})/T_b = E_{2\nu_3}/T_{2\nu_3} - E_{\nu_3}/T_{\nu_3}, \quad (7)$$

and

$$\delta = \exp(-E_{\nu_3}/kT_{\nu_3}) + 2 \exp(-E_{2\nu_3}/kT_{2\nu_3}), \quad (8)$$

or equivalently

$$\begin{aligned} N_{\nu_3}^e N_{\nu_3}^e / [N_{2\nu_3}^e (1 - N_{2\nu_3}^e - N_{\nu_3}^e)] \\ = \exp[(2E_{\nu_3} - E_{2\nu_3})/kT_b], \end{aligned} \quad (9)$$

and

$$\delta = N_{\nu_3}^e + 2N_{2\nu_3}^e, \quad (10)$$

where  $T_{\nu_x}$  is the vibrational temperature of mode  $\nu_x$ . Thus, assuming the kinetics are governed by eq. (6) from the reported temperature dependent amplitude ratios of the two exponentials in the  $\nu_3$  signal in ref. [2], we calculate a  $\delta = 0.25$  according to the above model (see fig. 4). It is important to note that the vibrational temperatures are mechanism dependent and they will change if a different model or additional states are considered in the kinetic system. It is, therefore, important to consider the possible participation of  $3\nu_3$  in the equilibration process and its effect on the vibrational temperatures of the system.

Since both  $\nu_3$  and  $2\nu_3$  are observed in the absorption spectra of the system, the first anharmonicity coefficient may be evaluated by assuming an equation of the form

$$G_{\nu_3}(v) = \omega_e(v + \frac{1}{2}) - \omega_e x_e(v + \frac{1}{2})^2,$$

where  $G_{\nu_3}(v)$  is the term value of the  $v$ th level of the  $\nu_3$  mode. Thus  $\omega_e = 1046 \text{ cm}^{-1}$  and  $\omega_e x_e = 8 \text{ cm}^{-1}$  for  $\text{CH}_3\text{F}$  in Xe. These are, as expected, quite close to the gas-phase values [5]. On the assumption that the anharmonicity term is not effected by the nature of the matrix,  $\omega_e = 1051 \text{ cm}^{-1}$  and  $\omega_e x_e = 8 \text{ cm}^{-1}$  for  $\text{CH}_3\text{F}$  in Kr. Thus the energy gaps for the following ladder climbing steps can be evaluated

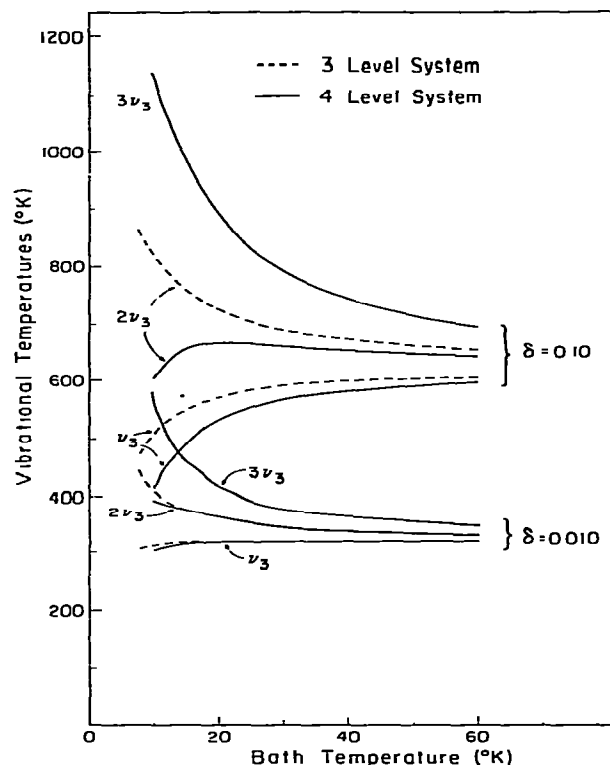


Fig. 4 The vibrational temperature of the  $\nu_3$  manifold is indicated as a function of bath temperature for two different levels of excitation ( $\delta$ ) and for a model which consists of either three levels (---) or four levels (—).



Both processes can proceed by the emission of a single phonon and are thus expected to be efficient. The absence of direct emission from  $3\nu_3$  to the ground state can be attributed to the highly non-allowed nature of the transition. This argument is supported by the fact that in the absorption spectra,  $2\nu_3$  could be readily observed but  $3\nu_3$  was not identified.  $3\nu_3$  may be incorporated in the model by assuming a bimolecular step for its population, similar to that of  $2\nu_3$ , as in eq. (12).

By a modification of eqs. (7)–(10) to include  $3\nu_3$  in the model, the vibrational temperatures of this four-level system can be solved for (see fig. 4). According to this model, a new value for  $\delta$ , namely 0.12, is calculated for the data reported in ref. [2].

These values for  $\delta$  in the above four-level model and the previously discussed three-level model seem large for the relatively mild excitation conditions in ref. [2] even considering that the exciting source was focused. Additionally, for similar matrix conditions, the reported fall rate to the fast exponential observed in ref. [2] for the  $\nu_3$  mode is slower than the rate of rise of  $2\nu_3$  that we observe for similar matrix conditions. Thus it may well be that other processes also contribute to the reported fast exponential fall such as filling of a hole burned in the matrix absorption line or as previously postulated, energy transfer to other sites [2].

It is important to note that if  $3\nu_3$  is populated by the above mechanism, it could funnel its population to the other states in the  $3000\text{ cm}^{-1}$  region ( $\nu_4$ ,  $2\nu_2$ ,  $2\nu_5$ ,  $\nu_1$ ) by sequential one- or two-phonon aided steps. However, such an "around the horn mechanism" has previously been shown to be inefficient in populating states lower in energy than the intermediate state ( $3\nu_3$ ) and the net effect of such a scheme, under the reported excitation conditions, could be to prevent the build up of population in  $3\nu_3$  and yet not significantly populate the neighboring modes on the timescale of deactivation [6].

The approximate expressions for  $N_{\nu_3}$  and  $N_{2\nu_3}$  [eqs. (5) and (6)] will breakdown for the case where either  $\delta$  is very large or  $k_r$  and  $k_l$  are similar in magnitude. In such an instance, the kinetics of the system is better treated by a numerical solution of the differential kinetic equations. The details and results of this treatment will be considered in a future publication. Nevertheless, the presented analytical solutions provide insight in the behavior of  $\nu_3$  and  $2\nu_3$  which is to be concisely considered below.

The rise rate of  $2\nu_3$  is expected to have a strong dependence on the bath temperature due to the microscopic reversibility relation between the forward and reverse rates of eq. (1)

$$k_{-1}/k_1 = \exp(-\Delta E/kT_b),$$

where  $T_b$  is the bath temperature. Additionally, as seen in eq. (6), the rise rate depends on  $N_{\nu_3}^e$  which in turn depends on the vibrational temperature of the system

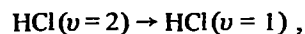
which, as discussed before, is dependent on  $\delta$ ,  $T_b$  and the specific model for the system's kinetics. Thus, studies of the temperature dependence and laser fluence dependence of the rise rate of  $2\nu_3$  could potentially discriminate between different models and yield  $k_1$ ,  $k_{-1}$  and an absolute measure of the absorption coefficient for the system. A dependence of rise rates on laser fluence has been observed and further studies of this, the temperature and spectral dependence of the rise rates in these systems are presently underway and will be reported on in a future publication. Indications are that on the time scale of the rise the kinetics may be more complicated than the model presented herein. However, on the timescale of the fall, the kinetics can be described by bimolecular interactions and the kinetic model we have developed should provide a starting point for the inclusion of more complex processes that may occur on the activation timescale.

Eq. (5) further implies that the deactivation rate of  $2\nu_3$  is quite independent of these parameters ( $T_b$  and  $\delta$ ). However, it should be noted that the mechanism of eq. (2) contains no allusion to a microscopic mechanism which in itself could contain a temperature dependence.

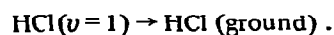
No laser fluence dependence is observed for the relaxation rate of  $2\nu_3$ , however, a well defined and reproducible dependence of the relaxation rate on matrix temperature is observed (fig. 3). As was done in the case of  $\text{CD}_3\text{F}$ , the temperature dependence of the relaxation rate can be reasonably well fit to the temperature dependence of the phonon population of a given energy phonon [7,8]. A  $36\text{ cm}^{-1}$  phonon in Kr and a  $28\text{ cm}^{-1}$  phonon in Xe result in relatively good agreement in each case. Perhaps more significant is the fact that the required phonon frequency to yield a reasonable fit in each case shifts in the same direction and with the same magnitude as the observed spectral shift of  $5\text{ cm}^{-1}$  between Kr and Xe. It is also interesting to note that this type of temperature dependence would be obtained if the relaxation process involved absorption of a phonon. In either case, the implication is that the rate determining step is that of an interaction between matrix and molecule through the phonon bath. With this reasoning it is not immediately apparent why the rate processes of activation and deactivation of  $\text{CH}_3\text{F}$  in Kr should be an order of magnitude greater than those of  $\text{CH}_3\text{F}$  in Xe.

Finally, it is important to note that in apparently similar investigations of CO [9], HCl and DCl [10],

many strikingly different results were obtained. The observed rates for the ladder climbing steps in these systems were reported to be  $\approx 3$  orders of magnitude smaller than those observed for  $\text{CH}_3\text{F}$ . In the CO system, the deactivation rates are, at least partially, radiatively controlled and the overtone was not observed to relax at twice the rate of the fundamental. In HCl and DCl studies, a sequential mechanism is postulated for the relaxation of the overtone of the type



followed by



Further experiments are underway to understand the reasons for the above differences and to try to fully elucidate the nature of energy transfer and relaxation processes for  $\text{CH}_3\text{F}$  in Kr and Xe matrices.

#### Acknowledgement

We would like to acknowledge the support of the donors of the Petroleum Research Fund administered by the American Chemical Society and the National Science Foundation under grant CHE79-08501. We would also like to thank the Northwestern University Material Research Center for aid in purchasing some of

the equipment used in this research under NSF Grant DMR-7-03019.

#### References

- [1] F. Legay, in *Chemical and biochemical applications of lasers*, Vol. 2, ed. C.B. Moore (Academic Press, New York, 1977); V.E. Bondybey and L.E. Brus, *Nonradiative Processes in Small Molecules in Low Temperature Solids*, *Advan. Chem. Phys.* (1980), to be published
- [2] L. Abouaf-Marguin, B. Gauthier-Roy and F. Legay, *Chem. Phys.* 23 (1977) 443.
- [3] B. Gauthier-Roy and L. Abouaf-Marguin, presented at the 6th International Conference on Molecular Energy Transfer, Rodez, France (July 1979).
- [4] R.K. Huddleston and E. Weitz, *J. Chem. Phys.* 66 (1979) 1740, C.E. Treanor, J.W. Rich and R.G. Rehm, *J. Chem. Phys.* 48 (1968) 1798.
- [5] S.M. Freund, G. Duxbury, M. Romheld, J.T. Tiedje and T. Oka, *J. Mol. Spectry.* 52 (1974) 38.
- [6] V.A. Apkarian and E. Weitz, *J. Chem. Phys.* 71 (1979) 4349.
- [7] B. Gauthier-Roy, L. Abouaf-Marguin and F. Legay, *Chem. Phys.* 46 (1980) 31.
- [8] M. Berkowitz and R.B. Gerber, *Chem. Phys.* 37 (1979) 369.
- [9] H. Dubost and R. Charneau, *Chem. Phys.* 12 (1976) 407.
- [10] J.M. Wiesenfeld and C.B. Moore, *J. Chem. Phys.* 70 (1979) 930.